

Multistep preparation into a single Zeeman sublevel in a ^{87}Rb vapor cell: Theory and experimentSalvatore Micalizio, Aldo Godone, Filippo Levi, and Claudio Calosso
Istituto Nazionale di Ricerca Metrologica (INRIM), Strada delle Cacce 91, 10135 Torino, Italy

(Received 24 March 2009; published 24 August 2009)

In this paper we propose a pumping scheme to concentrate nearly all the atoms of an alkali-metal vapor into one of the ground-state Zeeman sublevels. We report theory and experiment for the case of ^{87}Rb in a cell with buffer gas but the technique easily applies to other alkali-metal atoms. The pumping scheme consists of a suitable sequence of laser and microwave pulses after which a large fraction of atoms is transferred into the desired level. The efficiency of this technique depends mainly on the laser power and on the relaxation effects taking place inside the cell; in principle, more than 95% of the atoms can be prepared in a well-defined quantum state. Diagnostic of the resulting population distribution is made observing the free-induction decay signal at the output of a microwave cavity. This multistep laser-microwave pumping technique is particularly suited for compact vapor-cell frequency standards working in pulsed regime or in experiments where it is necessary to maintain the cylindrical symmetry of the experimental arrangement.

DOI: [10.1103/PhysRevA.80.023419](https://doi.org/10.1103/PhysRevA.80.023419)

PACS number(s): 32.80.Xx, 06.30.Ft, 32.30.Bv

I. INTRODUCTION

The possibility of preparing an atomic ensemble in a single sublevel of a Zeeman manifold or in a well-defined combination of quantum states is very attractive and desirable in many different atomic physics contexts. In atomic frequency standards, for example, preparing all the atoms in a single state with $m_F=0$ (one of the two clock levels) allows in general the observation of the atomic reference transition with a high contrast [1], while in quantum phase gate multi-level experiments initial ground-state populations need to be prepared in specific Zeeman sublevels (see, for example, [2]).

Several techniques have been successfully developed in this regard. It is well known, for example, that, in alkali-metal vapors, optical pumping with a pure circularly polarized light results in a concentration of the entire population in either $|F, m_F=-F\rangle$ or $|F, m_F=F\rangle$ level [3], except for the eventual effect of relaxation processes.

For atomic alkali-metal beams we mention the magnetic state selection, the simultaneous application of a magnetic or radio-frequency (rf) field and a pumping laser [4], and the use of at least two lasers with appropriate polarizations [5].

In [6] a method to prepare the spin state of a cold atomic ensemble trapped in a magneto-optical trap is demonstrated, while in [7] the case of a cesium vapor in a paraffin coated cell is studied.

The problem is more complex when the atomic sample is contained in a cell and diluted in a buffer gas since relaxation phenomena tend to rapidly equalize the populations among the sublevels.

In [8] Dehmelt suggested a method where the optical pumping is produced with narrow pulses of circularly polarized light propagating perpendicularly to the magnetic field. If the repetition rate of the light pulses is equal to the Zeeman resonance frequency, it is possible to increase the atomic population in $|F=2, m_F=0\rangle$ level, a very useful condition for clock operation. In fact, this method has been re-proposed by Davidovits and Novick [9] to produce an overpopulation of $|F=2, m_F=0\rangle$ level in the optically pumped

vapor-cell rubidium maser. Although this technique can in principle be applied to an alkali-metal vapor, the amount of atoms accumulated in the interested level is only slightly larger than that achievable with a regular optical pumping scheme; moreover, the method reported in [8] is hardly suitable in a cell-microwave cavity arrangement where in general pumping laser and quantization magnetic field are collinear.

The issue of putting nearly all atoms into a single $|F, m_F\rangle$ state of an atomic vapor has been discussed with some detail in a few works. In [10] a method is developed for a Rb cell with buffer gas in which a combination of laser and rf pulses is able to move the atomic population into the desired quantum state, while an all-optical technique is described in [11]. More recently, the possibility to pump a large fraction of atoms in a coherent superposition of states has been proved in [12] for a cell of alkali-metal atoms in a buffer gas, improving in this way the observation of coherent population trapping resonances.

In this work we devise a simple highly efficient pumping scheme applied to a ^{87}Rb vapor in a closed cell with buffer gas; this scheme consists of a suitable sequence of laser and microwave pulses for concentrating almost all the atoms in a Zeeman sublevel of the ground state. Quantization axis, pumping laser, and microwave field are all collinear in our scheme and consequently the cylindrical symmetry of the experimental apparatus is maintained. This is a key property when the cell needs, for example, to be placed in a microwave cavity or when the reduced size of the apparatus is a main concern, as for the implementation of compact vapor-cell clocks.

II. SCHEME

We consider a sample of ^{87}Rb atoms (nuclear spin $I=3/2$) in a cell with buffer gas (what follows is valid in general also for other alkali-metal atoms). The cell is placed in a microwave cavity resonant with the ground-state hyperfine transition (6834 MHz). The Zeeman degeneracy in the two ground-state hyperfine levels is resolved by applying a

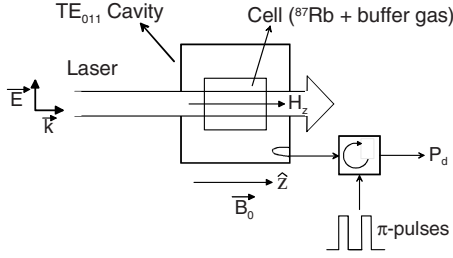


FIG. 1. Schematic setup for the multiple laser-microwave pumping scheme.

static magnetic field \vec{B}_0 that defines the z axis of a coordinate system, as shown in Fig. 1. The atoms are assumed to be initially in thermodynamic equilibrium then the atomic population in the ground state is equally distributed among the eight sublevels of $|5^2S_{1/2}\rangle$.

We face now the challenging problem to transfer with minimal losses the atomic population in one of the three sublevels with $F=1$ [see Fig. 2(a)]; we initially consider the $|F=1, m_F=0\rangle$ level that is particularly relevant for frequency standard applications. The first step to do that is to submit the

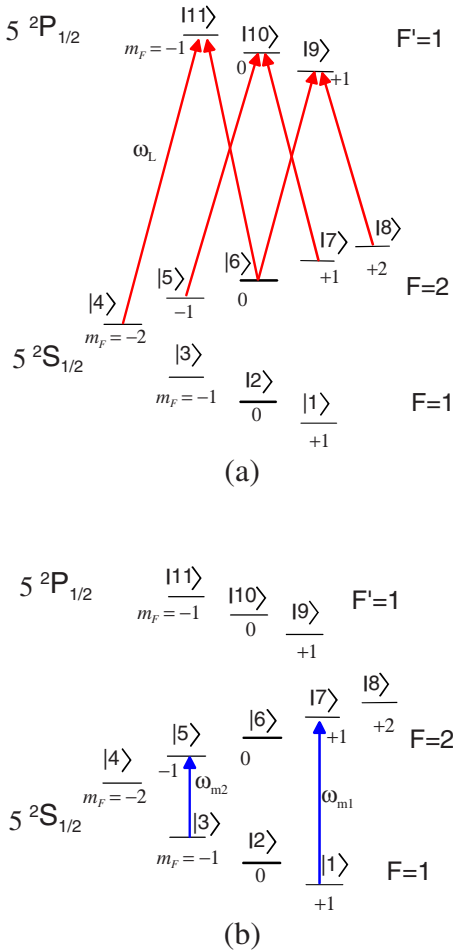


FIG. 2. (Color online) Multiple pumping sequence; (a) laser pulse at the end of which the atoms are equally distributed among the $F=1$ sublevels; (b) π microwave pulses to invert completely the atomic populations between the connected levels.

atoms to a strong laser pulse tuned to the $|5^2S_{1/2}; F=2\rangle - |5^2P_{1/2}; F'=1\rangle$ component of the D_1 optical transition. The laser is assumed to propagate in the z direction and to be linearly polarized. Due to selection rules, the atoms see the light as the combination of the two circular components σ^+ and σ^- , according to the scheme of Fig. 2(a) (incidentally, we note that the pumping scheme of Fig. 2(a) produces spin alignment; see, for example, [13]).

The laser pulse, of duration t_{p1} , changes the thermal equilibrium inside the ground state and will produce an imbalance between the two hyperfine multiplets. In particular, for a sufficiently high laser power at the end of t_{p1} all the atoms will move to level $|5^2S_{1/2}, F=1\rangle$, with a population distribution that we can suppose equal among the three sublevels. Therefore, no more than 1/3 of the total atomic population can be concentrated in the interested sublevel with a single laser pulse.

To transfer all the atoms into the desired sublevel, after switching off the laser, two microwave pulses resonant with the hyperfine transitions $|F=1, m_F=-1\rangle \leftrightarrow |F=2, m_F=-1\rangle$ and $|F=1, m_F=1\rangle \leftrightarrow |F=2, m_F=1\rangle$ are applied simultaneously to the atoms, as shown in Fig. 2(b). These microwave pulses should fulfill the following main requirements:

(i) The associated Rabi frequencies b_e satisfy the relation $b_e t_m = \pi$, where t_m is the microwave pulse duration [14]; we assume for simplicity equal b_e for both pulses. The goal of π pulses is to invert completely the populations of the connected levels so that the atoms that were initially concentrated in $|F=1, m_F = \pm 1\rangle$ are now transferred, respectively, to $|F=2, m_F = \pm 1\rangle$; no hyperfine coherence is generated in the atoms by π pulses.

(ii) $t_m \ll \gamma_1^{-1}$, where γ_1 is the total relaxation rate of the ground-state populations; in this way we can assume that the population of the $|F=1, m_F=0\rangle$ level does not change considerably during the time t_m .

(iii) According to selection rules for allowed transitions in low field, $\Delta F=1$ transitions with $\Delta m_F=0$ can take place if the microwave magnetic field and the quantization magnetic field are parallel [15]. In our case the TE_{011} cavity mode ensures this condition.

After the microwave pulses, the laser is again switched on for a time t_{p2} (that in general can be different from t_{p1}) and the atoms in levels $|F=2\rangle$, which have been repopulated by the couple of microwave pulses, are pumped again. The atoms experience then several of these alternating laser pumping-microwave pulse cycles until an equilibrium situation is achieved. We point out that the level $|F=1, m_F=0\rangle$ is the only one not connected to the externally applied fields so that the pumping scheme just described will concentrate the atoms into it.

To evaluate the amount of atoms that can be transferred to level $|F=1, m_F=0\rangle$ in this way, we refer to the model developed in [16]. The following physics is included in the model:

- (i) the full Zeeman manifold of the ground-state hyperfine levels;
- (ii) the dynamics induced by the relaxation phenomena in the distribution of the atomic populations;
- (iii) the absorption of the laser while propagating into the cell; and
- (iv) the spatial distribution of the electromagnetic field inside the cavity.

With respect to [16], we add the interaction with the two microwaves pulses. We study the effects of these physical phenomena by considering the evolution of the density matrix elements $\hat{\rho}$. We report here the general system of equations we solved and we refer to [16] for an extensive discussion of their validity,

$$\frac{\partial \rho_{11}}{\partial t} = D\nabla^2 \rho_{11} + \frac{1}{16}(\gamma_{1c} + \gamma_{1se})(-13\rho_{11} + 4\rho_{44} + \rho_{77} + 1) + \frac{\Gamma_p}{16} \left(\rho_{44} + \frac{1}{2}\rho_{77} + \frac{1}{6}\rho_{66} \right) + \text{Im}(\tilde{b}_e^* \delta_{17}),$$

$$\frac{\partial \rho_{44}}{\partial t} = D\nabla^2 \rho_{44} + \frac{1}{8}(\gamma_{1c} + \gamma_{1se})(3\rho_{11} - 4\rho_{44} + \rho_{77}) + \frac{\Gamma_p}{16} \left(-3\rho_{44} + \frac{1}{2}\rho_{77} + \frac{1}{6}\rho_{66} \right),$$

$$\frac{\partial \rho_{66}}{\partial t} = D\nabla^2 \rho_{66} - (\gamma_{1c} + \gamma_{1se})\rho_{66} - \frac{1}{8}(\gamma_{1c} + \gamma_{1se}) \times (3\rho_{11} + 4\rho_{44} + \rho_{77} - 2) + \frac{\Gamma_p}{16} \left(\rho_{44} + \frac{1}{2}\rho_{77} - \frac{7}{6}\rho_{66} \right),$$

$$\frac{\partial \rho_{77}}{\partial t} = D\nabla^2 \rho_{77} - \frac{1}{16}(\gamma_{1c} + \gamma_{1se})(3\rho_{11} + 4\rho_{44} + 17\rho_{77} - 3) + \frac{\Gamma_p}{16} \left(\rho_{44} - \frac{3}{2}\rho_{77} + \frac{1}{6}\rho_{66} \right) - \text{Im}(\tilde{b}_e^* \delta_{17}),$$

$$\frac{\partial \delta_{17}}{\partial t} = D\nabla^2 \delta_{17} - \frac{1}{32}(23\gamma_{1se} + 26\gamma_{1c})\delta_{17} + \frac{i}{2}\tilde{b}_e(\rho_{77} - \rho_{11}) - \frac{\Gamma_p}{32}\delta_{17},$$

$$\frac{\partial \Gamma_p}{\partial z} + \frac{1}{c} \frac{\partial \Gamma_p}{\partial t} = -\frac{\alpha}{\Gamma^*} \Gamma_p \frac{6\rho_{44} + 3\rho_{77} + \rho_{66}}{12},$$

$$\rho_{22} = 1 - 2\rho_{11} - 2\rho_{44} - 2\rho_{77} - \rho_{66} \quad \text{for each } t,$$

$$\tilde{b}_e(r, z) = b_e(r, z)e^{i\phi_e}, \quad b_e(r, z) = b_{e0} J_0\left(\frac{x'_{01} r}{a}\right) \cos\left(\frac{\pi z}{d}\right). \quad (1)$$

Here, we have the following:

- (i) ρ_{ii} ($i=1-8$) is the relative populations of the $|i\rangle$ th level; the levels are numbered as in Fig. 2.
- (ii) The microwave coherences are assumed to oscillate at the frequencies ω_{m1} and ω_{m2} of the externally applied fields: $\rho_{17} = \delta_{17} e^{i\omega_{m1} t}$ and $\rho_{35} = \delta_{35} e^{i\omega_{m2} t}$.
- (iii) D is the diffusion coefficient; γ_{1c} and γ_{1se} are the population relaxation rates due to buffer gas and spin exchange collisions, respectively; and Γ^* is the relaxation rate of the excited state.
- (iv) Γ_p is the optical pumping rate proportional to the laser intensity; it obeys the Maxwell equation for a laser field

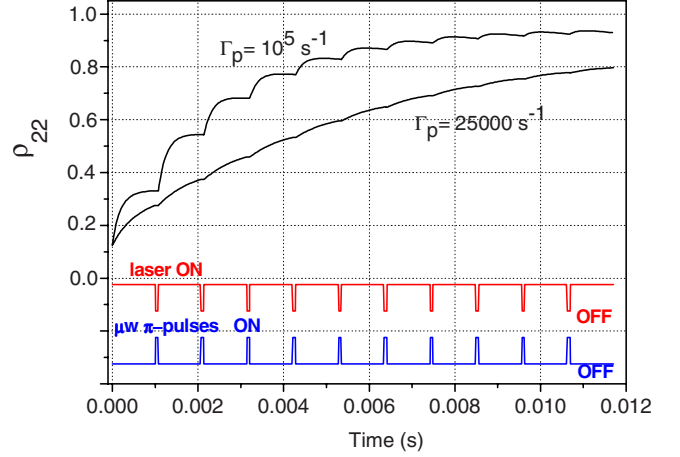


FIG. 3. (Color online) Calculated relative population of level $|2\rangle$ versus the pumping time for two values of the laser pumping rate; the bottom part of the figure shows the qualitative laser-microwave pulses timing sequence.

amplitude while propagating in a medium of linear absorption coefficient α and length L .

(v) \tilde{b}_e is the complex Rabi frequency associated to the microwave pulses, where ϕ_e is an arbitrary phase. In the definition of b_e we have made explicit the role of the spatial variables, b_e being proportional to the TE_{011} eigenvector cavity mode (x'_{01} is the first root of the derivative of the Bessel function $J_0(x)$ and a and d are the radius and the length of the cavity). b_{e0} is the value of the Rabi frequency in the center of the cell.

To write the previous set of equations we have exploited the symmetry of the excitation scheme and of the atomic level configuration that allows us to put $\rho_{33} = \rho_{11}$, $\rho_{88} = \rho_{44}$, $\rho_{55} = \rho_{77}$, and $\delta_{35} = \delta_{17}$ for each time, reducing the number of independent equations.

We point out that due to the field distribution and to the laser absorption, the atomic medium is not homogeneous. This means that not all the atoms are actually submitted to π pulses, in fact they will experience the microwave and laser field intensity according to their position inside the cell. However, according to the normalization of b_e , there will exist an optimum value of the product $b_{e0} t_m$ that maximizes the effect of population inversion averaged over the entire cell: we call this value π equivalent (π_{eq}).

During the laser pumping phase, no microwave is applied so that in the previous equations $b_e = 0$ and, similarly, when the atoms experience the microwave π pulses the laser pumping rate Γ_p is set to zero. The values assumed by the density matrix elements at the end of each phase settle the initial condition for the next step.

Figure 3 shows the calculated behavior of ρ_{22} resulting from this multiple laser-microwave pumping scheme; in the bottom part we have superimposed the relative pulse timing. The figure refers to a working temperature of $T_0 = 36^\circ\text{C}$, corresponding to an atomic density of $n \approx 3 \times 10^{10} \text{ cm}^{-3}$; under this condition the cell parameters have the following values (see [16]): $D = 8 \text{ cm}^2/\text{s}$, $\Gamma^* = 3 \times 10^9 \text{ s}^{-1}$, $\gamma_{1se} = 18.5 \text{ s}^{-1}$, $\gamma_{2se} = 11 \text{ s}^{-1}$, $\gamma_{1c} = 12 \text{ s}^{-1}$, and $\gamma_{2c} = 102 \text{ s}^{-1}$.

We observe that up to the 94% of population can be concentrated in this way into $|2\rangle$ for a $\Gamma_p = 10^5 \text{ s}^{-1}$. This value

results as a consequence of two opposite effects. On one hand, the multiple pumping scheme excites the atoms out of all $^2S_{1/2}$ levels except the desired one; the atoms that decay into it are not involved in the pumping process and ρ_{22} becomes larger and larger. But as the populations of the depleted levels become much smaller than $1/8$, relaxation phenomena tend to equilibrate the ground-state populations by taking out mainly the atoms from $|F=1, m_F=0\rangle$; the laser is no longer able to gain on relaxation and a balance between pumping rate and relaxation effects is established.

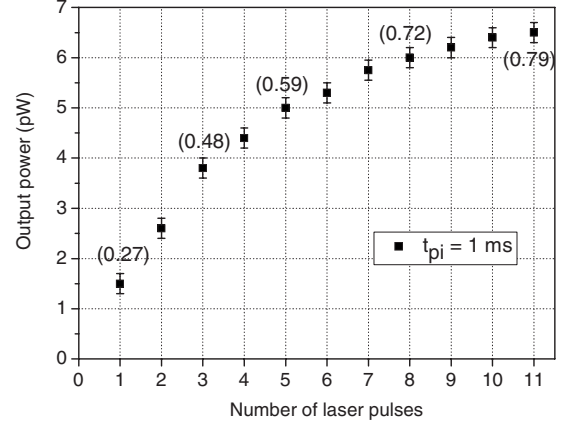
III. RESULTS

To demonstrate the effectiveness of the total pumping technique described so far, we apply it to a pulsed optically pumped (POP) ^{87}Rb passive maser. The experimental setup is described in detail in [17]; we recall here only the main elements. A diode laser is stabilized through an external ^{87}Rb reference cell to the 795 nm D_1 line of ^{87}Rb . The linearly polarized laser beam is sent to the physics package composed of a quartz cell and a high Q microwave cavity. At the input of the cell the laser intensity is about 2 mW/cm^2 , corresponding to a pumping rate of $\Gamma_p \approx 20\,000 \text{ s}^{-1}$. The cell contains the ^{87}Rb vapor and a mixture of buffer gases (Ar and N_2 in the pressure ratio of 1.6). The total buffer gas pressure is 25 Torr and the working temperature is $36.5 \text{ }^\circ\text{C}$. The sizes of the cell and of the cavity are those used for the computations previously reported. A quantization magnetic field of about 90 mG is applied to the atoms. To isolate the atoms from the fluctuations of the environmental magnetic field, the physics structure is placed inside two magnetic shields made in mu metal. The two hyperfine transitions are separated by $\pm 126 \text{ kHz}$ from the central 0-0 transition. These transitions are excited by means of two microwave pulses generated with the electronics described in [18]. The electronics is able as well to synchronize the different pumping phases, switching properly on and off laser and microwave; several sequences of alternating laser and microwave pulses similar to that of Fig. 2 may be produced. In particular, a sequence of up to 20 laser pulses and 19 couples of microwave pulses has been generated.

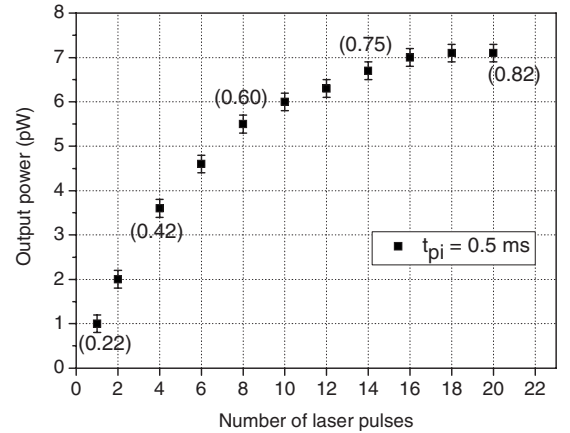
To prove the effectiveness of this pumping scheme, we observe the free-induction decay power P_d as detected at the cavity output after a $\pi/2$ pulse resonant with the $|F=1, m_F=0\rangle - |F=2, m_F=0\rangle$ clock transition [16],

$$P_d \propto \left(\int_{V_a} \Delta^p(r, z) \sin[b_e(r, z)t_m] H_{az}(r, z) dv \right)^2, \quad (2)$$

where V_a is the cell volume, $\Delta^p = \rho_{66} - \rho_{22}$ is the population difference reached at the end of the pumping phase, and H_{az} is the magnetic longitudinal field eigenvector [16]. We then use the direct link between P_d and ρ_{22} given by Eq. (2) to compare the experimental results with the theoretical predictions. We point out that the microwave pulse resonant with the 0-0 transition is applied only for diagnosis and not for



(a)



(b)

FIG. 4. (a) Measured microwave output power versus the number of laser pulses; each laser pulse lasts $t_{pi}=1 \text{ ms}$; (b) the same of (a) but for laser pulses of duration 0.5 ms each.

pumping purposes.

Figure 4 shows the measured power of the free-induction decay signal versus the number of laser pulses defining each sequence.

We indicated in parenthesis the amount of population concentrated in $|2\rangle$ averaged over the volume of the cell, as extrapolated from the solution of Eq. (1) and from Eq. (2). In particular, from Fig. 4(a) it turns out that we succeeded to concentrate up to the 80% of the atomic population in the desired level; each laser pulse for all the sequences is 1 ms long. A little more can be obtained with laser pulses of 0.5 ms long, as shown in Fig. 4(b), but in this case it is of course necessary a much larger number of steps. For both figures, each microwave pulse is $70 \text{ } \mu\text{s}$ long.

Another interesting topic to be addressed concerns the largest amount of atoms that can be placed in the desired level maintaining nearly constant the pumping time. In some applications it is in fact required to accumulate in one level the largest number of atoms in the shortest time. This is, for example, the case of pulsed vapor-cell clocks where it is important to prepare the largest fraction of atoms in one of the two clock levels, avoiding at the same time a significant increase in the cycle operation time.

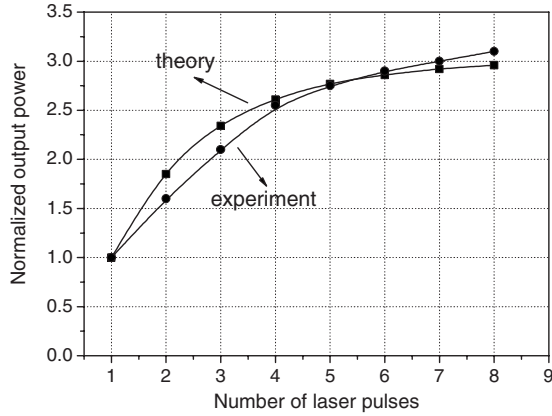


FIG. 5. Circles: measured output power versus the number of laser pulses for a total optical pumping of $t_p=4$ ms, $\Gamma_p=25\,000\text{ s}^{-1}$; squares: corresponding theoretical curve.

Figure 5 shows the measured microwave output power versus the number of laser pulses keeping the total optical pumping time equal to $t_p=4$ ms. In the case of n laser pulses, the length of each pulse is t_p/n . The measured power has been normalized to the value obtained by a single laser pulse of 4 ms. It turns out that with this multiple pumping scheme it is possible to obtain a signal up to three times larger than that achievable by a traditional optical pumping realized with a single laser pulse. The squares refer to the theoretical evaluation and are in very good agreement with the experimental points.

To further prove the effectiveness of the technique here described, we applied it to a POP clock prototype. The principle of operation of the POP clock is composed of three phases, as described in detail in [19]:

(i) a strong laser pulse pumps the atoms of $|F=2, m_F\rangle$ level, so that at the end of the laser pulse almost all the atoms are equally distributed in the three ground-state sublevels with $F=1$;

(ii) the atoms are then interrogated with two microwave pulses resonant with the clock transition $|F=1, m_F=0\rangle - |F=2, m_F=0\rangle$ of length t_m each, separated by a time T , according to the well-established Ramsey scheme; and

(iii) finally, a detection window is enabled so that the atoms that have made the clock transition are detected; in particular, in our case, the clock transition is detected through the free-induction decay signal observed after the second microwave pulse.

The conventional optical pumping phase made with a single laser pulse is replaced by the multistep technique here described and we compare the clock performance in the two situations. In particular, we measured the clock frequency stability in terms of Allan standard deviation [1] that is a significant parameter to characterize the performance of a vapor-cell clock. All the other operation phases (interrogation and detection of the clock transition) are identical in the two cases, as well as the values of the working parameters. The improvement of the clock stability due to the more efficient pumping technique is clearly observed in Fig. 6. The upper curve refers to a conventional optical pumping made with a single laser pulse of 4 ms, while the lower curve refers

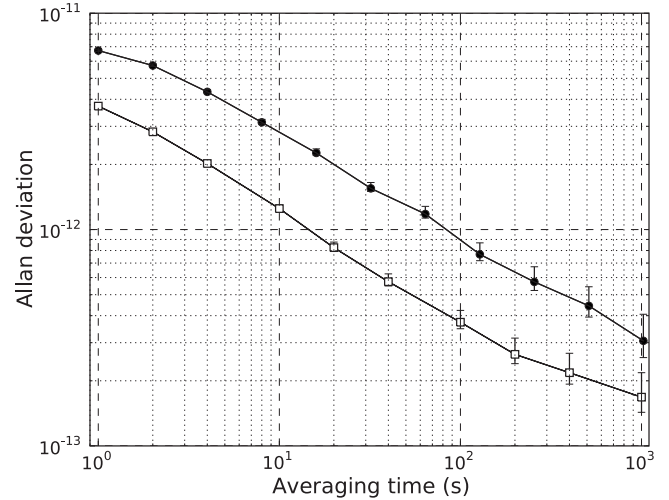


FIG. 6. Black circles: measured Allan deviation of the POP clock operating at $T_0=36.5\text{ }^\circ\text{C}$ with conventional pumping made with a single laser pulse; white squares: clock stability obtained with the multiple microwave-optical pumping. In this second case the stability improves since more atoms have been accumulated in the clock level during the pumping phase.

to a multistep optical-microwave pumping made with nine laser pulses of duration $444\text{ }\mu\text{s}$ each.

We have also performed experiments at $T_0=64\text{ }^\circ\text{C}$ obtaining again a good agreement between the theoretical predictions and the experimental results. In this case the gain due to the multistep laser-microwave pumping technique is lower than that obtained at $T_0=36.5\text{ }^\circ\text{C}$ due to the increased optical thickness of the atomic medium and to the increased effect of the relaxation phenomena (mainly spin exchange). In a pumping scheme similar to that of Fig. 5, it is however possible to concentrate up to 50% of the atomic population

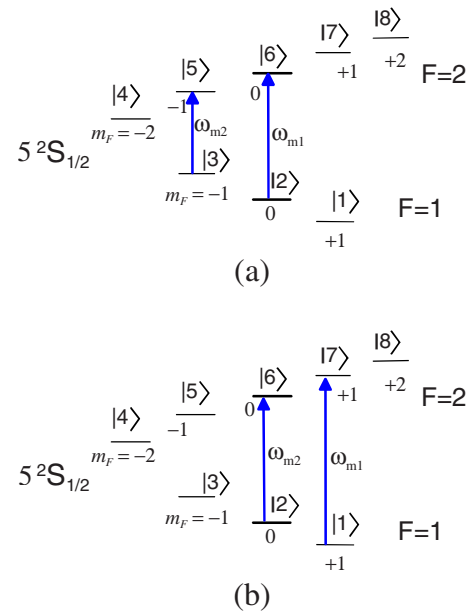


FIG. 7. (Color online) Other two possible microwave configurations to put the atoms in (a) level $|F=1, m_F=1\rangle$ or in (b) $|F=1, m_F=-1\rangle$.

in the desired level and the output power increases by a factor of 2 with respect to conventional optical pumping made with a single laser pulse.

Our scheme works as well for a wide range of buffer gas pressure. Increasing the buffer gas pressure requires an optimization of the number of laser pulses and of their duration in order to limit the effects of relaxation. Considering, for example, our buffer gas at a pressure of 100 Torr, a numerical simulation shows that it is possible to obtain a relative atomic population in the desired level of about 70% by using 15 laser pulses of duration 1.5 ms each and the same laser intensity of Fig. 4.

We point out that the proposed pumping scheme can be used to move the atoms in almost all the sublevels of the ground state. For example, once transferred the atoms in $|F=1, m_F=0\rangle$, a π -pulse resonant with the 0-0 transition can move them in $|F=2, m_F=0\rangle$. Moreover, the microwave pulses can be set as in Figs. 7(a) and 7(b); in this case the atomic population will concentrate, respectively, in levels $|F=1, m_F=1\rangle$ or $|F=1, m_F=-1\rangle$. Again, as done for the 0-0 transition, a further π pulse can move the atoms in $|F=2, m_F=1\rangle$ or $|F=2, m_F=-1\rangle$.

Incidentally, we recall that the density matrix can be expressed in terms of irreducible spherical tensor operators (see, for example, [20]). In this formalism, the physical situation in which all the atoms are in a single sublevel corresponds to a linear superposition of the spherical tensors of

rank $k=1$ (dipole polarization), $k=2$ (spin alignment), and $k=3$ (octupole polarization).

IV. CONCLUSION

In summary, in this paper we have demonstrated a multi-step laser-microwave pumping technique to prepare a large fraction of the ground-state ^{87}Rb atoms in a single Zeeman sublevel; in particular, we focused our discussion mainly on the $|F=1, m_F=0\rangle$ for its interest in the field of frequency standards and we proved that the fractional population difference $|\Delta| = |\rho_{66} - \rho_{22}|$ can be made as high as 0.6, resulting in a better signal-to-noise ratio of the clock signal; a significant improvement of the short-term frequency stability of the clock is then observed.

Numerical calculations elaborated from our theoretical model are in good agreement with the experimentally observed behavior; we are therefore confident that with a more powerful laser it is possible to concentrate up to 90% of the atoms in one single Zeeman sublevel of the ground state of ^{87}Rb . We point out that, of course, this method can be generalized to other atoms with $I > 3/2$, such as Cs or ^{85}Rb ; it is only necessary to excite the atoms with a proper number of microwave π pulses, leaving only the desired level uncoupled to the externally applied fields. This technique, besides being useful in atomic clocks, is of interest in all the applications that benefit from having the large possible fraction of atoms prepared in a well-defined quantum state, such as quantum computing and quantum state storage.

-
- [1] J. Vanier and C. Audoin, *The Quantum Physics of Atomic Frequency Standards* (Adam-Hilger, Bristol, 1989).
- [2] C. Ottaviani, D. Vitali, M. Artoni, F. Cataliotti, and P. Tombesi, Phys. Rev. Lett. **90**, 197902 (2003); Z.-B. Wang, K.-P. Marzlin, and B. C. Sanders, *ibid.* **97**, 063901 (2006).
- [3] W. E. Bell and A. L. Bloom, Phys. Rev. **107**, 1559 (1957); W. Happer, Rev. Mod. Phys. **44**, 169 (1972).
- [4] W. Dreves, H. Jansch, E. Koch, and D. Fick, Phys. Rev. Lett. **50**, 1759 (1983).
- [5] G. Avila, V. Giordano, V. Candelier, E. de Clercq, G. Theobald, and P. Cerez, Phys. Rev. A **36**, 3719 (1987); P. Tremblay and C. Jacques, *ibid.* **41**, 4989 (1990); B. P. Masteron, C. Tanner, H. Patrick, and C. E. Wieman, *ibid.* **47**, 2139 (1993).
- [6] B. Wang, Y. Han, J. Xiao, X. Yang, C. Zhang, H. Wang, M. Xiao, and K. Peng, Phys. Rev. A **75**, 051801(R) (2007).
- [7] B. Julsgaard *et al.*, J. Opt. B: Quantum Semiclassical Opt. **6**, 5 (2004).
- [8] H. G. Dehmelt, Bull. Am. Phys. Soc. **7**, 615 (1962).
- [9] P. Davidovits and R. Novick, Proc. IEEE **54**, 155 (1966).
- [10] N. D. Bhaskar, Phys. Rev. A **47**, R4559 (1993); IEEE Trans. Ultrason. Ferroelectr. Freq. Control **42**, 15 (1995).
- [11] J. Deng, in *Proceedings of the 2000 IEEE International Frequency Control Symposium*, edited by The IEEE Ultrasonics, Ferroelectrics, and Frequency Control Society (IEEE, Kansas, 2000), pp. 689–663.
- [12] Y.-Y. Jau, E. Miron, A. B. Post, N. N. Kuzma, and W. Happer, Phys. Rev. Lett. **93**, 160802 (2004); T. Zanon, S. Guerandel, E. de Clercq, D. Holleville, N. Dimarcq, and A. Clairon, *ibid.* **94**, 193002 (2005); A. V. Taichenachev, V. I. Yudin, V. L. Velichansky, A. S. Zibrov, and S. A. Zibrov, Phys. Rev. A **73**, 013812 (2006).
- [13] B. W. Shore, *The Theory of Coherent Atomic Excitation* (Wiley, New York, 1990), Vol. 2; J. D. Xu, G. Wackerle, and M. Mehring, Z. Phys. D: At., Mol. Clusters **42**, 5 (1997); A. Weis, G. Bison, and A. S. Pazgalev, Phys. Rev. A **74**, 033401 (2006).
- [14] Due to the inhomogeneity in the medium not all the atoms of the cell will experience actually π pulses; it is however possible to speak of π pulse as an equivalent averaged value all over the cell, as explained later in the text.
- [15] N. F. Ramsey, *Molecular Beams* (Oxford University Press, London, 1956).
- [16] S. Micalizio, A. Godone, F. Levi, and C. Calosso, Phys. Rev. A **79**, 013403 (2009).
- [17] A. Godone, S. Micalizio, F. Levi, and C. Calosso, Phys. Rev. A **74**, 043401 (2006).
- [18] C. Calosso, S. Micalizio, A. Godone, E. K. Bertacco, and F. Levi, IEEE Trans. Ultrason. Ferroelectr. Freq. Control **54**, 1731 (2007).
- [19] A. Godone, S. Micalizio, and F. Levi, Phys. Rev. A **70**, 023409 (2004).
- [20] A. Omont, Prog. Quantum Electron. **5**, 69 (1979).